Structural and magnetic properties of Fe and carbon nanotubes derived from coconut shells

Cite as: AIP Advances **8**, 055134 (2018); https://doi.org/10.1063/1.5025054
Submitted: 06 February 2018 . Accepted: 21 May 2018 . Published Online: 31 May 2018

S. B. Qadri, E. P. Gorzkowski, K. Bussmann, B. B. Rath, and J. Feng

AIP ADVANCES **8**, 055134 (2018)

Structural and magnetic properties of Fe and carbon nanotubes derived from coconut shells

S. B. Qadri,[a] E. P. Gorzkowski, K. Bussmann, B. B. Rath, and J. Feng
U. S. Naval Research Laboratory, Washington, DC 20375, USA

(Received 6 February 2018; accepted 21 May 2018; published online 31 May 2018)

Ferric oxide (Fe_2O_3) was directly reduced to metallic Fe using the carbon source from the coconut shells at temperatures above 1400 °C in argon gas atmospheres. X-ray diffraction analysis showed the presence of α-, γ- phases of Fe in addition to the presence of carbon nanotubes (CNTs). By selecting the appropriate ratios of coconut shell powder to Fe_2O_3, it is demonstrated that pure Fe is produced without any residual ferric oxide. The quantitative analysis of each of the Fe phases and carbon nanotubes was dependent on the temperature and the duration of processing at high temperature. Transmission electron microcopy results showed copious amount of carbon nanotubes in the samples. Magnetic property measurements suggested that, the average magnetic moment is consistent with presence of α-phase and the ferromagnetic γ-phase of Fe. This novel method of producing pure α- and γ-Fe in the presence of carbon nanotubes using coconut shells has potential applications as nanocomposites. https://doi.org/10.1063/1.5025054

INTRODUCTION

Iron is among the most abundant elements present on the Earth in much of its outer and inner core. Iron and its alloys have extensive applications ranging from magnetic, wear-resistant and corrosion resistance, and in variety of industries, such as the automotive, rail road gas transport and power generation, high strength alloys for many industrial applications, and many biological and medical applications.[1] Commercially, iron metal is produced by reduction of iron ore (ferric oxide) in blast furnaces, where ore is reduced by using coke into Fe having high carbon content, known as pig iron. The excess carbon is reduced using oxygen hearths followed by treatment to the carbon level necessary to make steel. Iron crystallizes in different phases under varying conditions of temperature and pressure. The thermodynamic phase diagram for pure iron indicates three different crystal structures as well as the liquid phase. Under the standard atmosphere pressure, iron exhibits the body centered cubic (bcc) crystal structure (α-Fe) from room temperature to 911 °C, the close-packed face centered cubic (fcc) structure (γ-Fe) between 911 °C and 1392 °C and the high-temperature bcc phase (δ-Fe) above 1392 °C until 1536 °C (the melting point), respectively. Under a pressure above about 13 GPa, the ε-Fe with a hexagonal close-packed (hcp) structure remains stable at 0 K. Martensite phase with a body centered tetragonal phase forms from austenite during a rapid quenching process. The formation of martensite phase involves a collective movement of atoms over less than an interatomic distance at a velocity approaching as high as that of sound. At ambient conditions, three allotropic forms are exhibited by Fe: bcc α-Fe also known as ferrite, FCC γ-Fe also known as austenite, and BCC δ-Fe which is the same as α-Fe except for reduced lattice parameter (2.866 Å for α-Fe versus 2.82 Å for δ-Fe). These different phases of iron dissolve different percentages of carbon 0.021% for α-Fe and up to 2.04% for γ-Fe.[2] On the other hand carbon nanotubes have unique electronic, magnetic and mechanical properties. They are orders of magnitude stronger than steel and yet very light in weight,

[a]syed.qadri@nrl.navy.mil

so nanotube fibers could be added to reinforce any material. They are unique because of the strong bonding between the carbon atoms. The graphene layer that makes up the nanotube appears to be like a rolled-up wire mesh with a network of hexagons joined together with carbon atoms at the apexes of the hexagons. Research is undergoing to use carbon CNTs for variety of medical applications involving detecting the cancerous cells and in delivering drugs to these cells.

There are two main kinds of agriculture's residues, one containing silica and organic matter and the other containing mostly organic matter without any significant amount of silica or other metallic impurities. Among the first type are rice husk, wheat husk, corn husk, sorghum leaves and peanut shells. Our previous work had demonstrated the utility of this type of agriculture residue in the synthesis of SiO_2, SiC, Si_3N_4, and zinc silicate by pyrolizing them in air, argon or in nitrogen atmospheres.[3–8] The second kind of agriculture residue which contains only organic matter, without any measurable silica content or metallic impurities include nut shells such as coconut, almond, walnuts, pistachio, macadamia, and cashew. Recently, it has been reported on the synthesis of CNTs derived from coconuts shells charcoal.[9,10] Billions of pounds of coconut shells, not biodegradable, go underutilized, which can be harnessed in the synthesis of a combination of Fe and carbon nanotubes.

The present study demonstrates, for the first time, a more effective and practical way of utilizing coconut shells as a carbon source mixed in the appropriate ratio with Fe_2O_3 (hematite) to produce

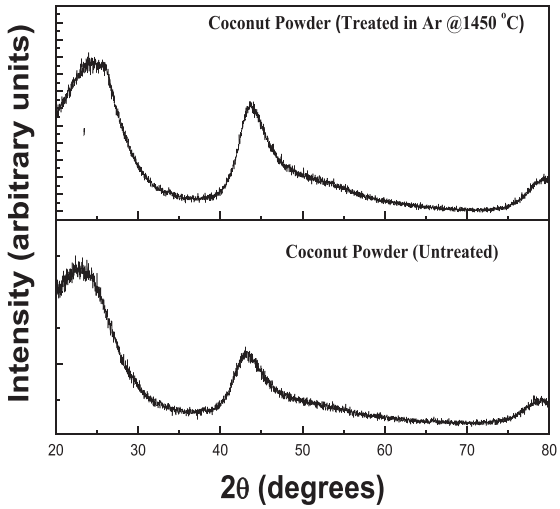

(a)

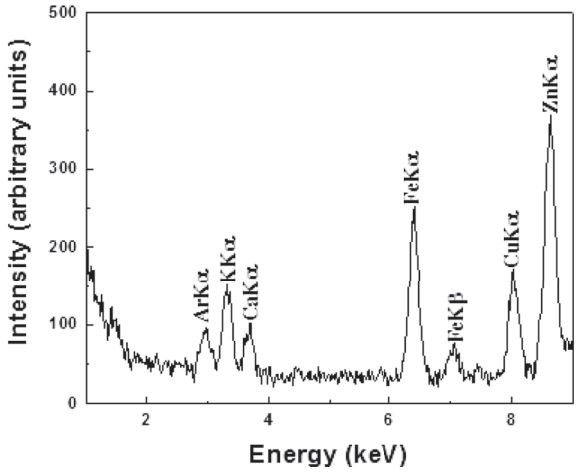

(b)

FIG. 1. (a) Overlay of XRD scans before and after heat treatment. (b) Energy dispersive x-ray fluorescence of coconut powder.

different phases of Fe with large quantities of carbon nanotubes, that will have potential medical and industrial implications. We have measured the magnetic properties of the samples and correlated the magnetic moments with the quantitative x-ray diffraction analysis of the Fe phases present in the samples. In addition, we have demonstrated a one single step process to obtain the large quantities of the carbon.

EXPERIMENTAL DETAILS

Samples were prepared from powders of raw nuts of coconuts by using ball milling with a SPEX 8000M including stainless steel milling media. The Fe_2O_3 sample along with the nut shell powder

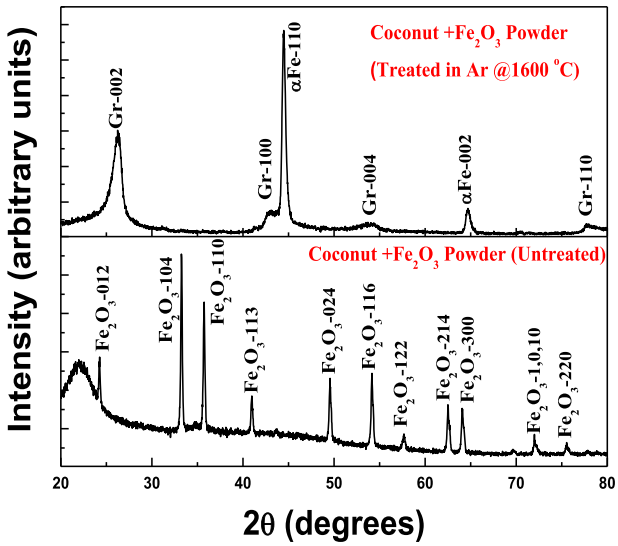

(a)

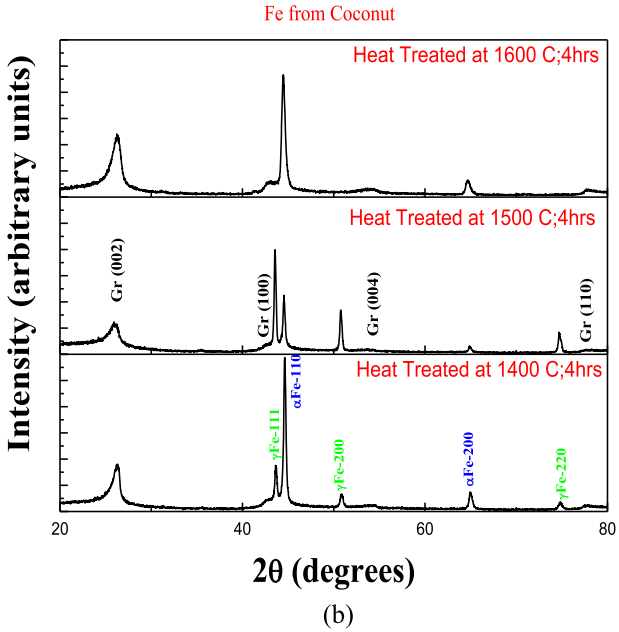

(b)

FIG. 2. (a) Comparison of XRD patterns of as prepared sample of coconut powder mixed with Fe_2O_3 showing peaks corresponding to α-phase of Fe_2O_3 and sample heat treated at 1600 °C showing peaks corresponding to only BCC α-phase of Fe and 2H-graphite peaks (CNTs) (b) Comparison of XRD patterns samples heat treated at 1400 °C, 1500 °C, and 1600 °C. The xrd scans for samples heat treated at 1400 °C and 1500 °C show mixed α- and γ-Fe phases.

was mixed thoroughly and then ball-milled to obtain a uniform powder. A hydraulic press was used to pressurize the homogenous powder filled in a die into 1 cm diameter disks with a 2.5-3 mm depth. The pellets were heat treated (pyrolised) in a convention furnace at temperatures exceeding 1400 °C for an interval of 5-6 hours in a dynamic argon atmosphere. XRD scans were obtained using a Rigaku 18 kW rotating anode generator and a high resolution powder diffractometer. The diffraction scans were collected using monochromatic CuKα radiation. Magnetic measurements were performed on a Digital Measurement Systems Technologies vibrating sample magnetometer (VSM). In order to conduct the TEM analysis, ethyl alcohol was mixed with the pyrolyzed sample; the mixture was then set in an ultrasonic cleaner. A carbon coated 200 mesh copper grid was submerged into the mixture to collect Fe and CNTs. A FEI Tecnai G2 TEM, operating at 300 kV was utilized to examine the sample.

RESULTS AND DISCUSSIONS

Figure 1a shows the x-ray diffraction scans of a coconut powder disc without any heat treatment and heat treated at 1450 °C in argon atmosphere for 4 hours. Both the scans show broad peaks characteristics of amorphous materials suggesting that heat treatment did not result in the formation of any crystalline phases. The x-ray fluorescence analysis spectrum of the coconut pellet (Figure 1b) shows the presence of trace elements of K, Ca, Fe, Cu and Zn. However, these trace amounts evaporates along with gases that were formed during the heat treatment and the processed sample did not show presence of any of these elements. Figure 2a shows an overlay of diffraction scans taken from coconut powder mixed with Fe_2O_3 in the weight ratio of 1:0.05 of coconut powder to Fe_2O_3 powder and heat treated samples at 1600 °C. The data for untreated sample consists of crystalline peaks corresponding to α-Fe_2O_3 and broad hump characteristics of amorphous material from the coconut powder. The diffraction peaks corresponding to Fe_2O_3 have been labeled and indexed on $R\bar{3}c$ rhombohedral phase with lattice parameters a=5.039 Å and c=13.740 Å consistent with the published values.[10] The scan from sample treated at 1600 °C shows peaks corresponding to 2H- graphite phase and the BCC α-Fe peaks. Figure 2b is an overlay of the x-ray diffraction scans taken from samples treated at 1400 °C, 1500 °C, and 1600 °C. The scans for 1400 °C and 1500 °C show the mixed phases of austenite (γ-phase) and α-ferrite phase of Fe in addition to peaks corresponding to graphite 2H- phase. All the diffraction scans were analyzed using Rietveld analysis to obtain quantitative weight percentages of each phase of Fe along with CNTs. The results are summarized in Table I.

The TEM micrographs for samples processed at 1400 °C, 1500 °C, and 1600 °C are given in Figures 3a, 3b and 3c. All the samples show the presence of large number of carbon nanotubes. The Fe nanoparticles are located inside as well as outside the CNTs. Based on the Rietveld quantitative analysis, assuming the Fe content to be 0.03497 gm for the starting mass of 0.05 gm of Fe_2O_3, the mass of the CNTs is approximately 0.14 gm for 1400 °C and 1500 °C samples with an estimated 0.08 gm of amorphous content, whereas the estimated content of the amorphous phase annealed at 1600 °C to be zero.

The magnetic measurements, M vs H for the three samples are given in Fig. 4a, 4b and 4c. The saturation magnetization for 1400 °C and 1500 °C samples is reduced, compared to the one

TABLE I. Lattice parameters and quantitative analysis of CNTs and Fe phases.

Sample Temp °C/Time	Final Wt.	Cryst. Size (nm)	α-phase	γ-phase	Graphite
0.05gm Fe_2O_3 + 1.0 gm 1400/4hrs	0.255gm	49 (α-Fe) 41 (γ-Fe)	2.868 Å 14.8%	3.588 Å 5.5 %	a = 2.448 Å; c = 6.767 Å 79.7%
0.05gm Fe_2O_3 + 1.0 gm 1500/4 hrs	0.260 gm	44 (α-Fe) 63 (γ-Fe)	2.868 Å 6.4%	3.587 Å 14.8%	a = 2.443 Å; c = 6.767 Å 78.8%
0.05gm Fe_2O_3 + 1.0 gm 1600/4 hrs	0.25 gm	27 (α-Fe)	2.886 Å 12 %	-	a = 2.458 Å; c = 6.802 Å 88%

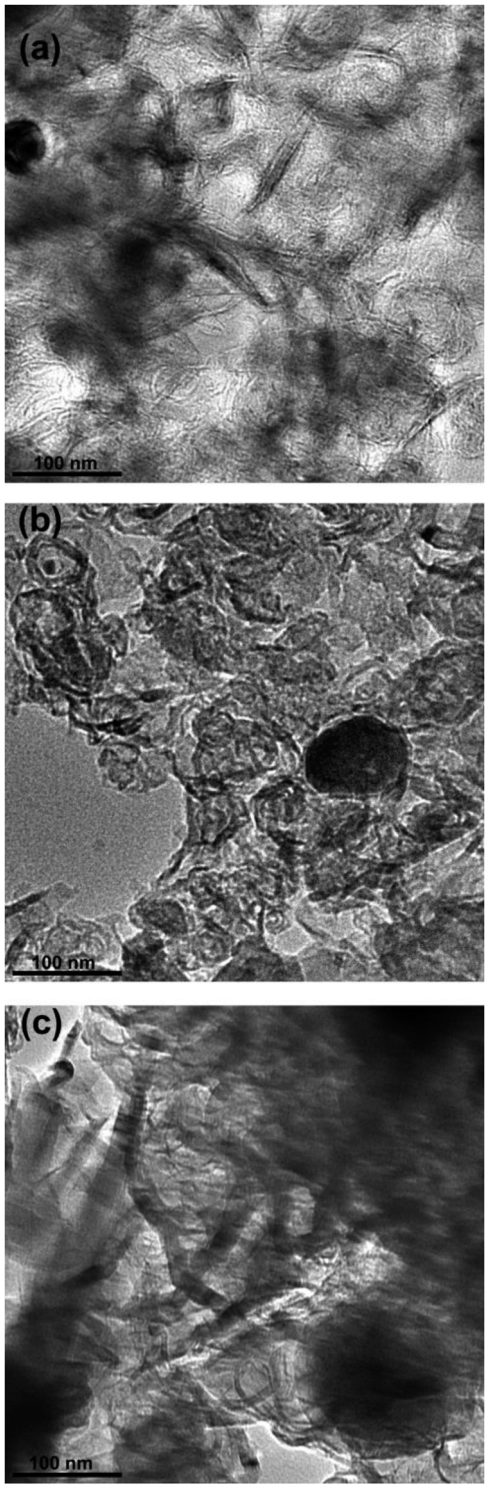

FIG. 3. TEM micrographs of samples heat treated at 1400 °C, 1500 °C, and 1600 °C showing the presence of CNTs.

at 1600 °C sample. Based on the x-ray measurements the 1600 °C sample consists of α-Fe phase only and using the mass of the Fe in the sample the magnetic moment is calculated as 220 emu/gm or 2.2 μ_B (Bohr Magnetons) consistent with literature value. However, for 1400 °C and 1500 °C samples, which has mixed phases of α- and γ-Fe phases, the moments were determined by using the

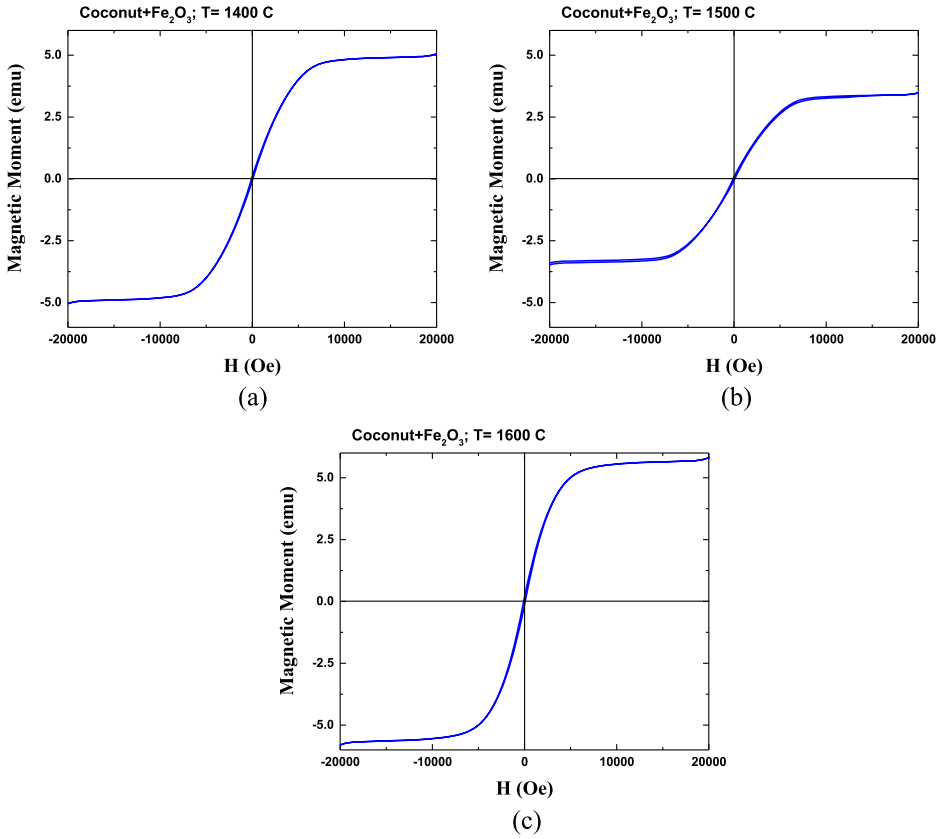

FIG. 4. M vs H curves for samples heat treated at 1400 °C, 1500 °C, and 1600 °C showing that the saturation magnetization decreased for 1400 °C, 1500 °C samples.

weight % of each phases as determined from x-ray Rietveld analysis and solving the simultaneous equations. The results show the moments to be 210 emu/gm or 2.10 μ_B for α-phase and 77 emu/gm or 0.77 μ_B for the γ-Fe phase. These measurements suggested γ-Fe to be ferromagnetic with a low moment of 0.77 μ_B.

The relative weight percentages of α- and γ-Fe phases is consistent with Fe-C phase diagram which shows that at 1500 °C more of γ-phase is formed when compared to α-Fe. However, the stability of γ-phase at room temperature is consistent with the presence of excessive carbon. Based on theoretical predictions, the FCC γ-Fe can have three phases including non-magnetic, an antiferromagnetic state, and low and high moment in the ferromagnetic state.[11,12] It is also estimated by extrapolating high temperature data, the lattice parameter is 3.59 Å. Our measurements showed a lattice parameter with 3.585 Å with a low moment of 0.77 μ_B.

CONCLUSIONS

The following three conclusions can be drawn from the present studies:

(1) Pure coconut shells (without any additives) and when heat treated above 1400 °C in argon atmosphere show only amorphous carbon.
(2) Coconut shells mixed with Fe_2O_3, heat treated in argon atmosphere results in the formation of pure α- and γ-Fe phases with large quantities of CNTs annealed at 1400 °C and 1500 °C. Samples showed only α-Fe phase with large quantities of CNTs when heated to 1600 °C.
(3) Magnetic data showed α-Fe to have magnetic moment of 220 emu/gm or 2.2 μ_B whereas the γ-Fe to be ferromagnetic with a moment of 77 emu/gm or 0.77 μ_B consistent with theoretical prediction.

[1] N. Gunkelmann, E. M. Bringa, K. Kang, G. J. Ackland, C. J. Ruestes, and H. M. Urbassek, "Polycrystalline iron under compression: Plasticity and phase transitions," Phys. Rev. B **86**, 144111 (2012).
[2] T. Lee, M. I. Baskes, S. M. Valone, and J. D. Doll, "Atomistic modeling of thermodynamic equilibrium and polymorphism of iron," J. Phys.: Condens. Matter **24**, 225404 (2012).
[3] S. B. Qadri, A. Fliflet, M. A. Imam, B. B. Rath, and E. P. Gorzkowski, "Silicon carbide synthesis from agricultural waste," USPatent 20130272947 A1 (2013).
[4] S. B. Qadri, A. Fliflet, M. A. Imam, B. B. Rath, and E. P. Gorzkowski, "Silicon carbide synthesis," (2013) US20140287907 A1.
[5] S. B. Qadri, E. P. Gorzkowski, M. A. Imam, A. Fliflet, R. Goswami, H. Kim, and B. B. Rath, Industrial Crops and Products **51**, 158–162 (2013).
[6] S. B. Qadri, E. P. Gorzkowski, B. B. Rath, J. Feng, S. N. Qadri, H. Kim, and M. A. Imam, J. Appl. Phys. **117**, 044306 (2015).
[7] S. B. Qadri, B. B. Rath, E. P. Gorzkowski, J. Wollmershauser, and C. Feng, J. Appl. Phys. **118**, 104904 (2015).
[8] S. B. Qadri, M. Imam, A. Fliflet, B. B. Rath, R. Goswami, and J. Caldwell, J. Appl. Phys. **111**, 073523 (2012).
[9] A. Melati and E. Hidayati, Journal of Physics: Conf. Series **694**, 012073 (2016).
[10] R. Araga and C. S. Sharma, Mater. Lett. **188**, 205 (2017).
[11] C. S. Wang, B. M. Klein, and H. Krakauer, Phys. Rev. Lett. **54**, 1852 (1985).
[12] A. S. Edelstein, C. Kim, S. B. Qadri, K. H. Kim, V. Browning, H. Y. Yu, B. Maruyama, and R. K. Everett, Solid State Comm. **76**, 1379 (1990).